J. Cell. Mol. Med. Vol 14, No 12, 2010 pp. 2803-2815

Zoledronic acid repolarizes tumour-associated macrophages and inhibits mammary carcinogenesis by targeting the mevalonate pathway

Marta Coscia [a, b, #, *], Elena Quaglino [c, #], Manuela Iezzi [d], Claudia Curcio [c], Francesca Pantaleoni [b], Chiara Riganti [e], Ingunn Holen [f], Hannu Mönkkönen [g], Mario Boccadoro [a], Guido Forni [c], Piero Musiani [d], Amalia Bosia [e], Federica Cavallo [c, #], Massimo Massaia [a, b, #]

[a] Divisione di Ematologia dell'Università di Torino, Azienda Ospedaliero Universitaria S. Giovanni Battista di Torino, Torino, Italy
[b] Laboratorio di Ematologia Oncologica, Centro di Ricerca Medicina Sperimentale (CeRMS), Azienda Ospedaliero Universitaria S. Giovanni Battista di Torino, Torino, Italy
[c] Molecular Biotechnology Center, Department of Clinical and Biological Sciences, University of Torino, Torino, Italy
[d] Aging Research Center, Department of Oncology and Neuroscience, 'G. D'Annunzio' University of Chieti-Pescara, Chieti, Italy
[e] Dipartimento di Genetica, Biologia e Biochimica, Università di Torino, Torino, Italy
[f] Academic Unit of Clinical Oncology, School of Medicine and Biomedical Sciences, University of Sheffield, Sheffield, UK
[g] Department of Pharmaceutics, University of Kuopio, Kuopio, Finland

Received: March 31, 2009; Accepted: September 18, 2009

Abstract

It is unknown whether zoledronic acid (ZA) at clinically relevant doses is active against tumours not located in bone. Mice transgenic for the activated ErbB-2 oncogene were treated with a cumulative number of doses equivalent to that recommended in human beings. A significant increase in tumour-free and overall survival was observed in mice treated with ZA. At clinically compatible concentrations, ZA modulated the mevalonate pathway and affected protein prenylation in both tumour cells and macrophages. A marked reduction in the number of tumour-associated macrophages was paralleled by a significant decrease in tumour vascularization. The local production of vascular endothelial growth factor and interleukin-10 was drastically down-regulated in favour of interferon-γ production. Peritoneal macrophages and tumour-associated macrophages of ZA-treated mice recovered a full M1 antitumoral phenotype, as shown by nuclear translocation of nuclear factor κB, inducible nitric oxide synthase expression and nitric oxide production. These data indicate that clinically achievable doses of ZA inhibit spontaneous mammary cancerogenesis by targeting the local microenvironment, as shown by a decreased tumour vascularization, a reduced number of tumour-associated macrophages and their reverted polarization from M2 to M1 phenotype.

Keywords: zoledronic acid • mevalonate pathway • tumour-associated macrophages • angiogenesis • tumour microenvironment

Introduction

Nitrogen-containing bisphosphonates (NBPs) are potent inhibitors of osteoclast-mediated bone resorption with proven efficacy in the treatment of cancer patients with bone metastases [1]. NBPs inhibit the active site of the enzyme farnesyl pyrophosphate (FPP) synthase in the mevalonate (Mev) pathway, resulting in reduced levels of isoprenoids required for the prenylation of GTPase signalling proteins essential for normal cellular function and survival [2, 3]. The Mev pathway is the only source of isoprenoids in mammalian cells, meaning that NBPs have the potential to affect the survival and function of many cell types other than osteoclasts, including macrophages, dendritic cells, endothelial cells and tumour cells [4–8]. Zoledronic acid (ZA) is the most potent NBP clinically available due to its double nitrogen group [3]. *In vitro* data have shown that ZA exerts a direct proapoptotic activity on tumour cells and reduces their adhesion, migration and invasion

[#]These authors contributed equally to this work.
*Correspondence to: Marta COSCIA,
Divisione di Ematologia dell'Università di Torino,
Azienda Ospedaliero Universitaria S. Giovanni Battista di Torino,
Via Genova 3, 10126, Torino, Italy.
Tel.: 00 39 0116336728
Fax: 00 39 0116963737
E-mail: marta.coscia@unito.it

doi:10.1111/j.1582-4934.2009.00926.x

potential [2, 9]. ZA has also indirect antitumour effects *via* its anti-angiogenic [7, 10, 11] and immunomodulatory properties [6, 8, 12, 13]. In view of its high affinity for mineralized bone, *in vivo* tumour models have mostly addressed the ability of ZA to reduce the skeletal tumour burden or bone metastasis. Few studies have investigated the activity of ZA against tumours not located in bone. In these studies ZA was used at doses exceeding those recommended in the clinical practice [9–11, 14–16]. Clinically compatible doses have been used in a mouse model xenografted with human breast cancer cells [17], but this study investigated bone metastasis rather than primary tumour development and did not take the role of the local microenvironment and the immune system into account. Whether or not ZA at clinically achievable doses can exert antitumour activity in tumours not located in bone is thus an unresolved issue. We have addressed this issue by investigating the effect of ZA at clinically compatible doses in mice transgenic for the activated form of rat ErbB-2 (neu) oncogene (BALB-neuT mice) [18]. These mice develop metastatic tumours with a stepwise progression very similar to that of human breast cancer [19]. To gain further insight into the mechanisms underlying any antitumour activity, we have also investigated whether ZA at clinically achievable concentrations can modulate the Mev pathway and protein prenylation in tumour cells and macrophages.

Materials and methods

Mice

BALB-neuT female mice were bred for us under specific pathogen-free conditions by Charles River (Calco, Italy) and treated according to the guidelines established in Principles of Laboratory Animal care (directive 86/609/EEC). Mice were randomly assigned to the control and treated groups, both investigated concurrently. Mammary pads were inspected weekly to monitor the appearance of palpable tumour masses. Masses with a mean diameter of $\geq$1 mm were regarded as tumours. Growth was monitored until all 10 mammary glands displayed a tumour or until a tumour exceeded a mean diameter of 10 mm, at which time mice were killed for humane reasons. The percentage of mice without tumour in function of time in weeks was evaluated to assess tumour-free survival. Tumour multiplicity was calculated as the cumulative number of incident tumours per total number of mice and is reported as the mean $\pm$ S.E.M. To assess tumour growth rate the diameter of each growing tumour was evaluated once a week and reported as the mean tumour diameter $\pm$ S.E.M. The percentage of mice alive in function of time in weeks was evaluated to assess overall survival.

BALB-neuT mice knocked out (KO) for the interferon-γ (IFN-γ) gene (BALB-neuT/IFN-γ KO) [20] were generated by crossing BALB-neuT mice with BALB/c mice KO for IFN-γ gene from The Jackson Laboratory (Bar Harbor, ME, USA).

ZA administration

Starting at 7 weeks of age, BALB-neuT mice received repeated courses of saline (control mice) or 100 μg/kg of ZA (Novartis Farma, Origgio, Italy) injected intravenously (i.v.) once a week for 4 weeks. This course was repeated after 3 weeks of rest throughout their life.

Morphological analysis and whole mount preparation

After two courses of saline or ZA, three mice from each group were killed and their mammary tissue morphologically analysed. Mice pelts were fixed for 4 hrs in periodate-lysine paraformaldehyde (PLP), washed in phosphate-buffered saline (PBS) containing 20% of sucrose, processed for whole mount preparations, performed as indicated in http://ccm.ucdavis.edu/tgmouse/ HistoLab/wholmt1.htm, and stained with ferric haematoxylin. Images were taken with a Nikon Coolpix 990 digital camera (Nital Spa, Torino, Italy) mounted on a stereoscopic MZ 6 microscope (Leica Microsystems, Milano, Italy) [21]. Two mammary glands from each animal were embedded in OCT (Bio-Optica Spa, Milano, Italy) and sectioned at 4 μm for histological and immunohistochemical studies.

Cells

TUBO cells are a cloned line derived from a mammary tumour of a BALB-neuT female [22] and N11 glial cells are a macrophage-like mouse cell line [23]. They were grown in Dulbecco modified Eagle medium (DMEM) (BioWhittaker Europe, Verviers, Belgium) supplemented with 20% foetal bovine serum (FBS) (Invitrogen Life Technologies, San Giuliano Milanese, Italy), and incubated at 37°C in a humidified 5% CO_2 incubator.

Peritoneal macrophages were obtained from 18-week-old untreated or ZA-treated mice (*in vivo* ZA treated) by washing the peritoneal cavity with 10 ml cold PBS containing 500 I.U. of heparin (Mayne Pharma, Neaples, Italy). In ZA-treated mice the treatment schedule was the same as for other experiments. The cell suspension was centrifuged, plated in a 6-well flat-bottom plate and allowed to adhere for 4 hrs. Then, wells were washed three times with medium RPMI (Roswell Park Memorial Institute) 1640 (Invitrogen Life Technologies) supplemented with 10% FBS (Invitrogen Life Technologies) to remove non-adherent cells. Peritoneal macrophages from untreated mice were cultured for 24 hrs in the absence (control) or in the presence of ZA 1 μM (*ex vivo* ZA-treated).

Isoprenoids and cholesterol synthesis

TUBO cells, and control, *ex vivo* or *in vivo* ZA-treated peritoneal macrophages were incubated for 24 hrs with 1 μCi of [^{3}H]acetate (3600 mCi/mmol; Amersham International, Bucks, UK). The intracellular synthesis of FPP, ubiquinone and cholesterol was measured by methanol/hexane extraction method, as previously described [24]. To detect the intracellular isopentenyl pyrophosphate (IPP) cells were lysed in ice-cold acetonitrile containing 100 mM $NaVO_4$ as reported [3], and resolved by thin layer chromatography. Standard solutions of FPP, ubiquinone, cholesterol and IPP were employed to identify each isoprenoid species. After the separation, the radioactivity of each spot was measured by liquid scintillation counting and expressed as fmol/1 $\times$ 10^6 cells (for cholesterol, FPP and ubiquinone) and as pmol/1 $\times$ 10^6 cells (for IPP), according to the titration curve previously obtained.

Ras prenylation and Ras activity assays

A band shift assay was used to evaluate Ras prenylation [25] in TUBO cells, control peritoneal macrophages and *ex vivo* or *in vivo* ZA-treated peritoneal

macrophages. Briefly, cells were lysed in 300 μl RIPA buffer (40 mM Tris-HCl, 150 mM NaCl, 0.1% SDS, 0.5% sodium deoxycholate, 1% Triton X-100, 0.1 mM ethylenediaminetetraacetic acid [EDTA]; pH 7.5), supplemented with the protease inhibitor cocktail set III (Calbiochem, La Jolla, CA, USA). Twenty μg total cell lysate were separated on a 10–20% precast Novex Tris-Glycine gel (Invitrogen Life Technologies), transferred on a PVDF membrane sheet (Immobilon-P, Millipore, Bedford, MA) and probed with a mouse monoclonal anti-Ras antibody (diluted 1:2000 in TBS-milk 3%, Millipore).

Ras activity was measured by a pull-down assay to detect the Ras-GTP binding, as previously described [26]. Cells were lysed in MLB buffer (125 mM Tris-HCl, pH 7.4, 750 mM NaCl, 1% Nonidet P40, 10% glycerol, 50 mM MgCl2, 5 mM EDTA, 25 mM NaF, 1 mM NaVO4, 10 μg/ml leupeptin, 10 μg/ml pepstatin, 10 μg/ml aprotinin and 1 mM PMSF) and centrifuged at 13000 g for 10 min. at 4°C. Protein content and total Ras were determined on an aliquot of supernatant. Thirty μg of the supernatant were incubated for 45 min. at 4°C with the Ras Assay Reagent (containing the Raf-1 Ras Binding Domain, agarose conjugate, Millipore). The beads were washed three times in MLB buffer and harvested by the addition of 20 μl Laemmli buffer (125 mM Tris, 4% w/v SDS, 20% v/v glycerol and 1% β-mercaptoethanol). Samples were resolved by 12% SDS-PAGE and Western blotting, using the anti-Ras antibody.

In vitro proliferation assay

TUBO cell proliferation was measured with the Cell proliferation ELISA, 5-bromo-2-deoxyuridine (BrdU) kit (Roche Molecular Biochemicals; Mannheim, Germany) following the manufacturer's instruction. After 24 hrs of seeding to obtain 80% confluence, 1×10^5 TUBO cells in 200 μL of DMEM with 20% FBS were incubated without ZA or with 1, 10 or 100 μM ZA in a humidified 5% CO_2 incubator. The ELISA assay was performed at 8, 48, 96 and 102 hrs, and adsorbance was measured with an automated Biorad 680 XR microplate reader (Bio-Rad Laboratories, Milano, Italy).

Histology and Immunohistochemistry

For the morphological analysis cryo-sections were stained with haematoxylin & eosin or with immunohistochemical assays and evaluated by two pathologists blind to treatment group. For the detection of infiltrating immune cells, cytokines and growth factors, slides were incubated for 30 min. with primary antibodies anti-CD11c (dendritic cells), -Mac1 (macrophages), -Gr-1 (granulocytes), -B220 (B cells), -TCRγδ (gamma delta T cells), -CD31 (endothelial cells) (all from BD Biosciences Pharmingen, Italy), -CD4 ($CD4^+$ T cells), -CD8a ($CD8^+$ T cells), -interleukin-10 (IL-10), -IFN-γ (all from Abcam plc, Cambridge, UK), -Foxp3 (T regulatory cells) (e-Bioscience, Inc., San Diego, CA, USA), -vascular endothelial growth factor (VEGF) (Santa Cruz Biotechnology, Santa Cruz, CA, USA) and -nitrotyrosine (as marker for peroxynitrite formation *in vivo*) (Invitrogen Life Technologies). After incubation with the appropriated secondary antibodies staining was developed with neutravidin-alkaline phosphatase conjugated (Thermo Scientific, Waltham, MA, USA) or Streptavidin peroxidase (Lab Vision, Fremont, CA, USA).

Western blot analysis

Control peritoneal macrophages and *ex vivo* or *in vivo* ZA-treated peritoneal macrophages were solubilised in the lysis buffer (25 mM Hepes, 135 mM NaCl, 1% Nonidet P-40, 5 mM EDTA, 1 mM EGTA, 1 mM $ZnCl_2$, 50 mM NaF and 10% glycerol). Thirty micrograms of total cell proteins were separated by SDS-PAGE and probed with antibodies to the inducible form of nitric oxide synthase (NOS-II, iNOS) (1:500), IκBα (1:250), 3-phosphate dehydrogenase (anti-GAPDH, 1:500) (all from Santa Cruz Biotechnology). Mouse N11 glial cells incubated for 24 hrs with 20 μg/ml of bacterial lipopolysacharide (LPS) were used as positive control.

Electrophoretic mobility shift assay (EMSA)

The activation of nuclear factor (NF)-κB was measured in the nuclear extracts of control peritoneal macrophages and *ex vivo* or *in vivo* ZA-treated peritoneal macrophages, as previously described [27]. Mouse N11 glial cells incubated for 24 hrs with 20 μg/ml LPS were used as positive controls.

Nitrite production

Nitrite production was measured in the supernatant from control peritoneal macrophages and *ex vivo* or *in vivo* ZA-treated peritoneal macrophages as previously described [28] and was expressed in nmol nitrite/mg cell proteins.

Statistical analyses

All data were analysed with the use of the software Graph Pad Prism, version 5.01 (GraphPad Software Inc., La Jolla, CA, USA). Differences in tumour free and overall survival were evaluated with the log-rank (Mantel-Cox) Test. Group comparisons were made by Student's two-tailed t-test. A *P*-value of 0.05 or less was considered as a significant difference.

Results

ZA impairs the onset and growth of ErbB-2-driven carcinomas

ZA was administered i.v. to BALB-neuT mice starting at 7 weeks of age. On average, mice received 16 ZA injections (range 12 to 22). As compared to control mice, ZA-treated mice displayed a significant extension in the median tumour-free survival (Fig. 1A), a significant reduction in tumour multiplicity (Fig. 1B), a significant delay in the tumour growth rate (Fig. 1C), and a significant prolongation of survival. At 28 weeks of age, 86% of ZA-treated mice were still alive when all control mice were dead (Fig. 1D).

This antitumour effect was an early event already evident after the first two courses of ZA. Numerous large opacities corresponding to hyperplastic lesions and solid tumour masses were evident in the mammary glands from control mice (Fig. 1E), whereas ZA-treated mice showed mammary glands with very

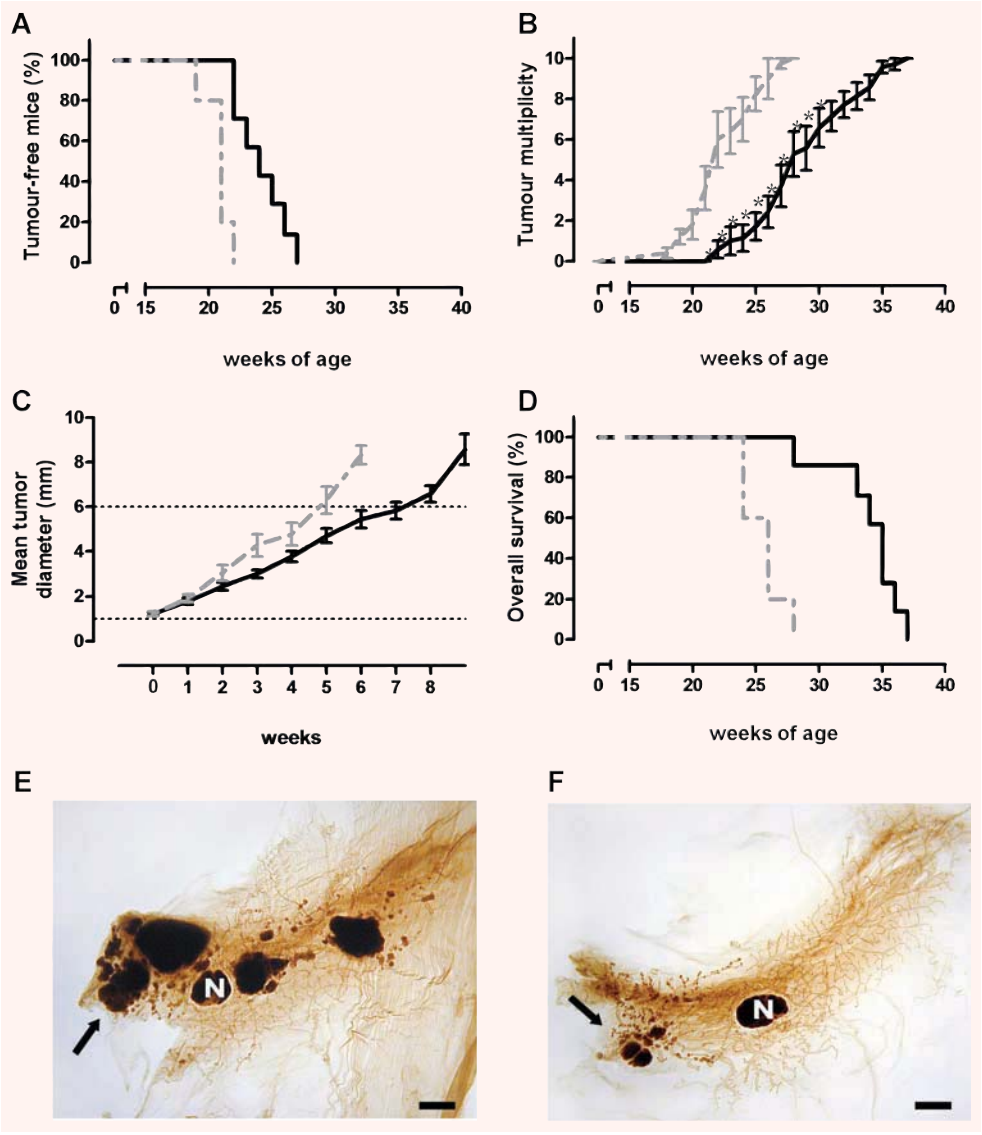

Fig. 1 ZA administration hampers ErbB-2 driven mammary carcinogenesis. Seven-week-old BALB-neuT female mice started to receive weekly i.v. courses of ZA 100 μg/kg (black line, $n = 7$) or saline (dotted grey line, $n = 5$). (**A**) Mice receiving i.v. ZA displayed a significant extension in the median tumour-free survival ($P = 0.0004$, log-rank, Mantel-Cox test) (24.5 weeks *versus* 19 weeks, $P < 0.0004$, Student's t-test), as compared to control mice. (**B**) ZA antitumour effect on tumour multiplicity resulted in a statistically significant reduction of the mean number of tumours from week 21 to week 30 ($P = 0.002$, Student's t-test). (**C**) ZA antitumour effect on carcinoma growth rate. The mean tumour diameter of each control and ZA-treated mice was evaluated in function of weeks. A statistically significant prolongation of time required by ZA-treated tumours to grow from 1 to 6 mm was observed (30.4 ± 1.8 days *versus* 41.1 ± 2.0 days; $P = 0.001$, Student's t-test). (**D**) ZA-treated mice displayed a significant extension in the median overall survival ($P = 0.0009$, Log-rank, Mantel-Cox test) as compared to control mice. (**E**, **F**) whole mount images of representative 18-week-old BALB-neuT mammary glands from control (e) and ZA-treated (f) mice. Several large tumour masses were evident in control mice, whereas fewer and smaller early-stage lesions, mostly confined to the nipple area, were observed in ZA-treated mice. Black arrows indicate foci of carcinomas. N = mammary lymph node. Scale bar, 2 mm.

few, small neoplastic lesions confined to the tissue close to the nipple (Fig. 1F).

ZA efficacy in hampering spontaneous lung metastasis was also evaluated [29]. Thirty-week-old ZA-treated mice displayed a significant reduction in the size of metastatic areas as compared to control mice (Fig. S1).

No evidence of tissue toxicity was detected by histological examination in kidney or other tissues (Fig. S2), whereas an increase of bone density by CT scanning was detected in ZA-treated mice (Fig. S3).

Low-dose ZA inhibits the Mev pathway of TUBO cells

TUBO cells were incubated with ZA at concentrations of 1 μM, 10 μM and 100 μM. The former concentration was selected by extrapolation from the pharmacokinetic data of cancer patients receiving the equivalent standard clinical dose, because mice treated with ZA at 100 μg/kg are expected to have serum concentrations close to ZA 1 μM [9]. The higher concentrations were selected as positive controls, because ZA at these doses blocks the Mev pathway and exert

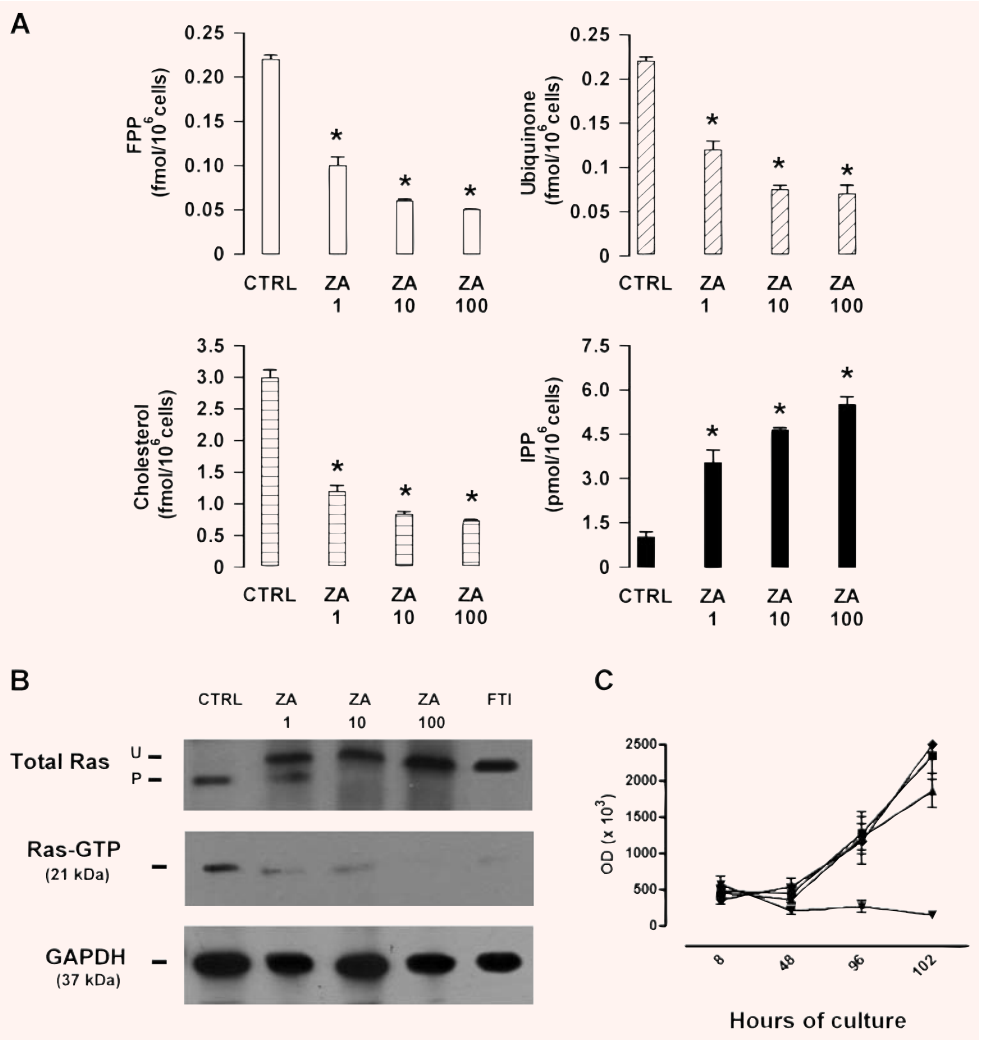

Fig. 2 Clinically compatible doses of ZA inhibits the activity of the Mev pathway, but not the proliferative rate of TUBO cells *in vitro*. (**A**) ZA induces a dose-dependent inhibition of FPP synthase in TUBO cells, as shown by the significant intracellular reduction of FPP, ubiquinone and cholesterol, and the significant increase of IPP (*P*-values from <0.02 to <0.001 for all ZA concentrations, Student's t-test). Results are expressed as the mean ± S.E.M. of three independent experiments. (**B**) Western blot analysis of prenylated (P) and unprenylated (U) Ras and pull-down assay for Ras-GTP in TUBO cells cultured in the absence (CTRL), or in the presence of 1, 10 and 100 μM ZA. The specific farnesyl transferase inhibitor (FTI) 277 (10 μM) was used as a positive control of Ras inhibition. The expression of GAPDH was used as a control of equal protein loading. Results are from one representative out of three experiments. (**C**) ZA inhibition of TUBO cells proliferation was assessed by measuring BrdU incorporation. TUBO cells were incubated in quadruplicates without ZA (◆) or with ZA at 1 μM (■), 10 μM (▲) or 100 μM (▼). BrdU incorporation was measured after 8, 48, 96 and 102 hrs as the mean optical density measured for each quadruplicate. As shown, ZA 1 μM never affected tumour cell proliferation, whereas 10 μM ZA induced a time-dependent inhibition and 100 μM ZA a complete abrogation of BrdU incorporation. Results are expressed as mean ± S.E.M. of three experiments.

direct proapoptotic and antiproliferative effects on tumour cells [30]. TUBO cells cultured for 24 hrs with 1 μM ZA displayed a significant reduction in cholesterol, ubiquinone and FPP, and a significant increase of IPP (Fig. 2A). These changes further increased upon incubation with 10 μM and 100 μM ZA, confirming a dose-dependent effect on the Mev pathway.

A band shift assay was performed to evaluate the effect of ZA on Ras prenylation. In untreated TUBO cells, the prenylated (P) form of Ras was largely predominant, whereas in ZA-treated TUBO cells the unprenylated (UP) form of Ras emerged and became largely predominant at 10 and 100 μM ZA concentrations. Western blot analysis showed that Ras-GTP levels, the active form of P Ras [26], were decreased in a dose-dependent manner in ZA-treated cells. TUBO cells incubated with the specific farnesyl transferase inhibitor FTI-277 served as controls in this set of experiments (Fig. 2B).

To assess whether ZA could have a direct effect on tumour cells, a proliferative assay was performed on TUBO cells cultured *in vitro* for 5 days in the presence of ZA 1, 10 or 100 μM. Although ZA 1 μM did not affect BrdU incorporation, a significant inhibition was observed when TUBO cells were cultured with 10 and 100 μM ZA. This inhibition became evident after 48 hrs and peaked after 5 days (Fig. 2C).

These data indicate that low concentrations of ZA inhibit the Mev pathway and Ras prenylation, but lack a direct antitumour activity against TUBO cells.

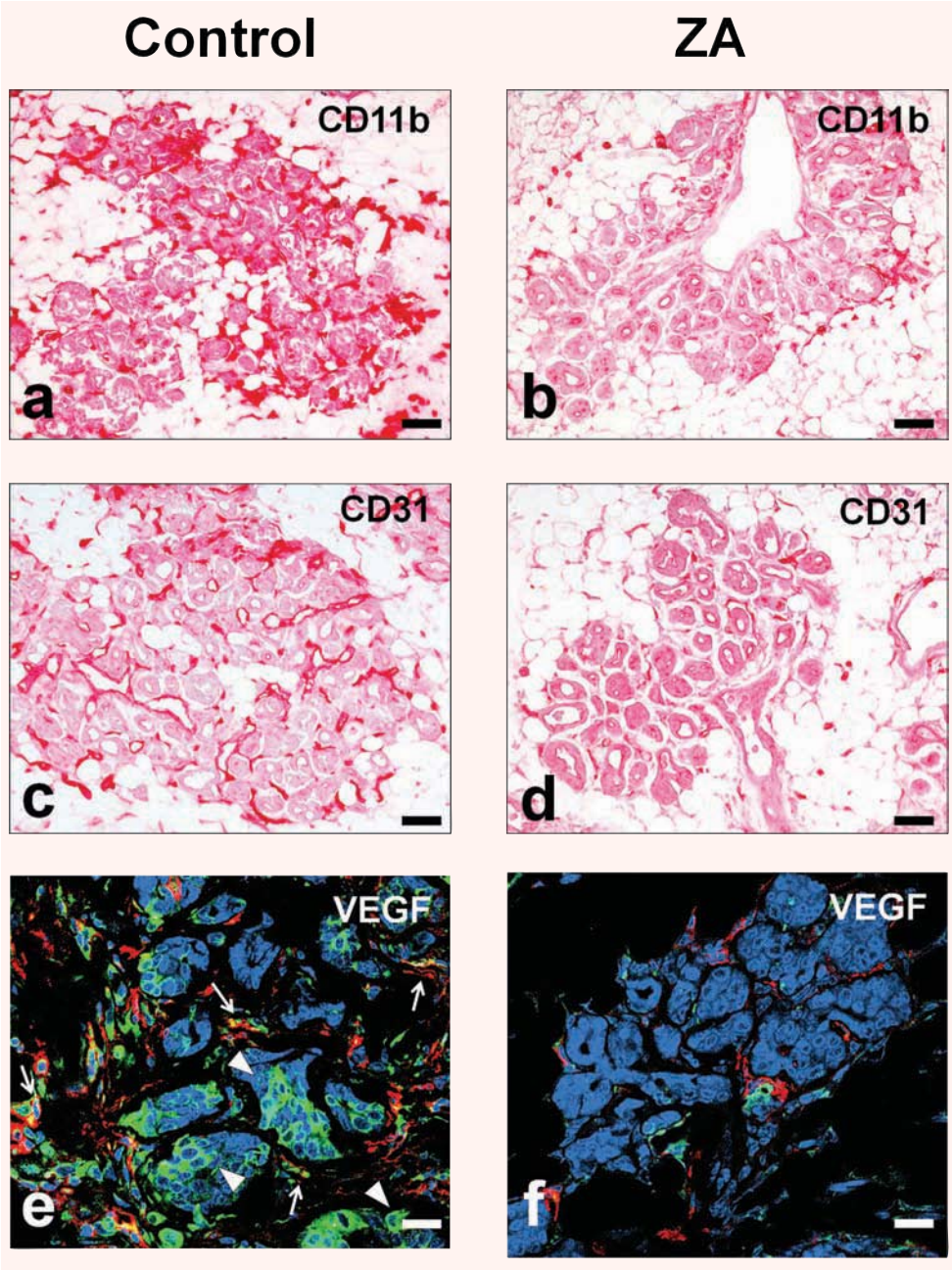

Fig. 3 ZA impairs TAM recruitment, angiogenesis and VEGF release at the tumour site. Immunohistochemical analysis of the tumour site showed a strong reduction in interstitial CD11b$^+$ TAMs in ZA-treated (**B**) as compared to control mice (**A**). CD31 immunostaining showed substantial neovascularisation in 18-week-old control mice (**C**), which was clearly inhibited by ZA treatment (**D**). Reduced VEGF expression was detected in TAMs of ZA-treated mice (**F**) as compared to control mice (**E**), as revealed by colocalization of VEGF (green) and CD11b (red). A strong reduction in the amount of VEGF produced by tumour cells was also observed in ZA-treated mice as compared to control mice. Arrowheads indicate some of the VEGF expressing tumour cells. Arrows indicate some of the VEGF expressing TAMs. Scale bars, 80 μm.

ZA impairs tumor-associated macrophages (TAMs) recruitment and tumour vascularization

The tumour stroma of control and ZA-treated mice did not show any significant difference in the number of infiltrating CD4 and CD8 T lymphocytes, B lymphocytes, regulatory T cells, granulocytes and γδ-T cells (data not shown), with the striking exception of CD11b$^+$ macrophages. These cells heavily infiltrated the stroma of early tumours in control mice (Fig. 3A). This recruitment was paralleled by intense angiogenesis around mammary ducts displaying tumoral lesions (Fig. 3C). By contrast, both the number of infiltrating CD11b$^+$ macrophages (Fig. 3B) and that of blood vessels associated with the mammary lesions (Fig. 3D) were strongly reduced in ZA-treated mice.

Immunohistochemical analysis showed that both tumour-associated macrophages (TAMs) and tumour cells stained positively for intracytoplasmic VEGF in control mice (Fig. 3E). Conversely, the decrease in TAMs density was paralleled in

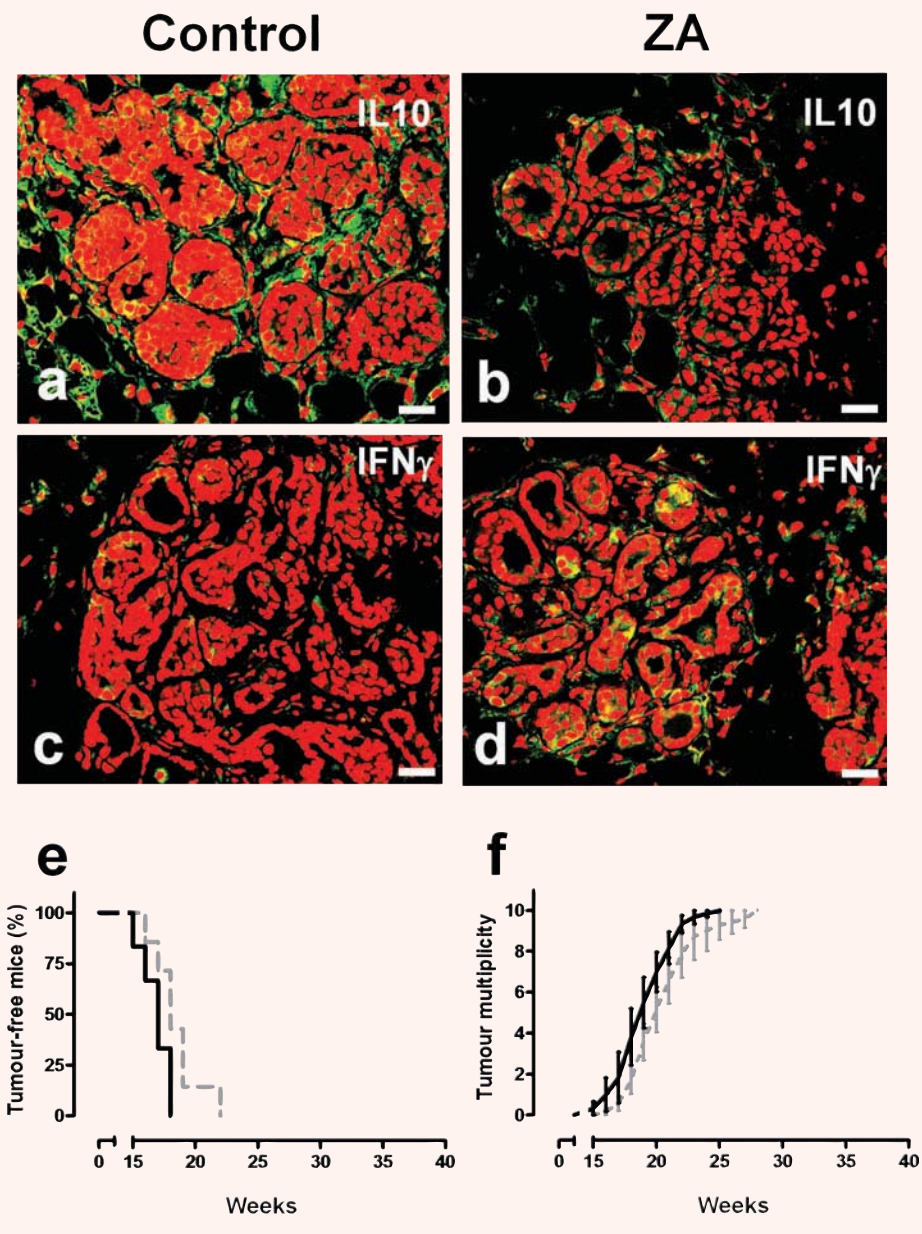

Fig. 4 ZA's antitumour effect is associated with its ability to reverse TAM polarization from M2 to M1, and is dependent on IFN-γ. Immunohistochemical analysis of representative mammary glands of 18-week-old control (**A**, **C**) *versus* ZA-treated (**B**, **D**) BALB-neuT mice. (**A**, **B**) Anti IL-10 staining (green) showed a clear reduction of IL-10 release in the tumour microenvironment of ZA-treated mammary tumours. (**C**, **D**) A significant enhancement of IFN-γ release (green) is observed in the microenvironment of ZA-treated mammary tumours. Scale bars, 40 μm. (**E**, **F**) ZA antitumour activity in BALB-neuT/IFN-γ KO. BALB-neuT/IFN-γ KO female mice received weekly i.v. courses of ZA (black line, $n = 6$) or saline (dotted grey line, $n = 7$). ZA-treated BALB-neuT/IFN-γ KO mice displayed the same tumour incidence (**E**) and tumour multiplicity (**F**) as control mice.

ZA-treated mice by a strong reduction of TAMs and tumour cells positively stained for VEGF (Fig. 3F). The reduced production of VEGF at the tumour site in ZA-treated mice was paralleled by a significant decrease in the serum level of VEGF (Fig. S4).

Repolarization of TAMs from M2 to M1 phenotype in ZA-treated mice

As VEGF plays a key role in inducing a M2 polarization of TAMs [31, 32], we evaluated whether the decrease of VEGF observed in the tumour microenvironment of ZA-treated mice was associated with a recovered M1 functional program. Indeed, TAMs of 18-week-old control mice expressed IL-10 (Fig. 4A) but not IFN-γ (Fig. 4C), whereas TAMs of ZA-treated mice stained negative for IL-10 (Fig. 4B), and became strongly positive for IFN- γ (Fig. 4D).

The weight of this IFN-γ induction was functionally assessed in BALB-neuT/IFN-γ KO mice. These mice showed the same tumour-free survival (Fig. 4E) and the same tumour multiplicity (Fig. 4F) as their control littermates despite ZA treatment, endorsing the role of IFN-γ in the ZA-induced impairment of tumour progression.

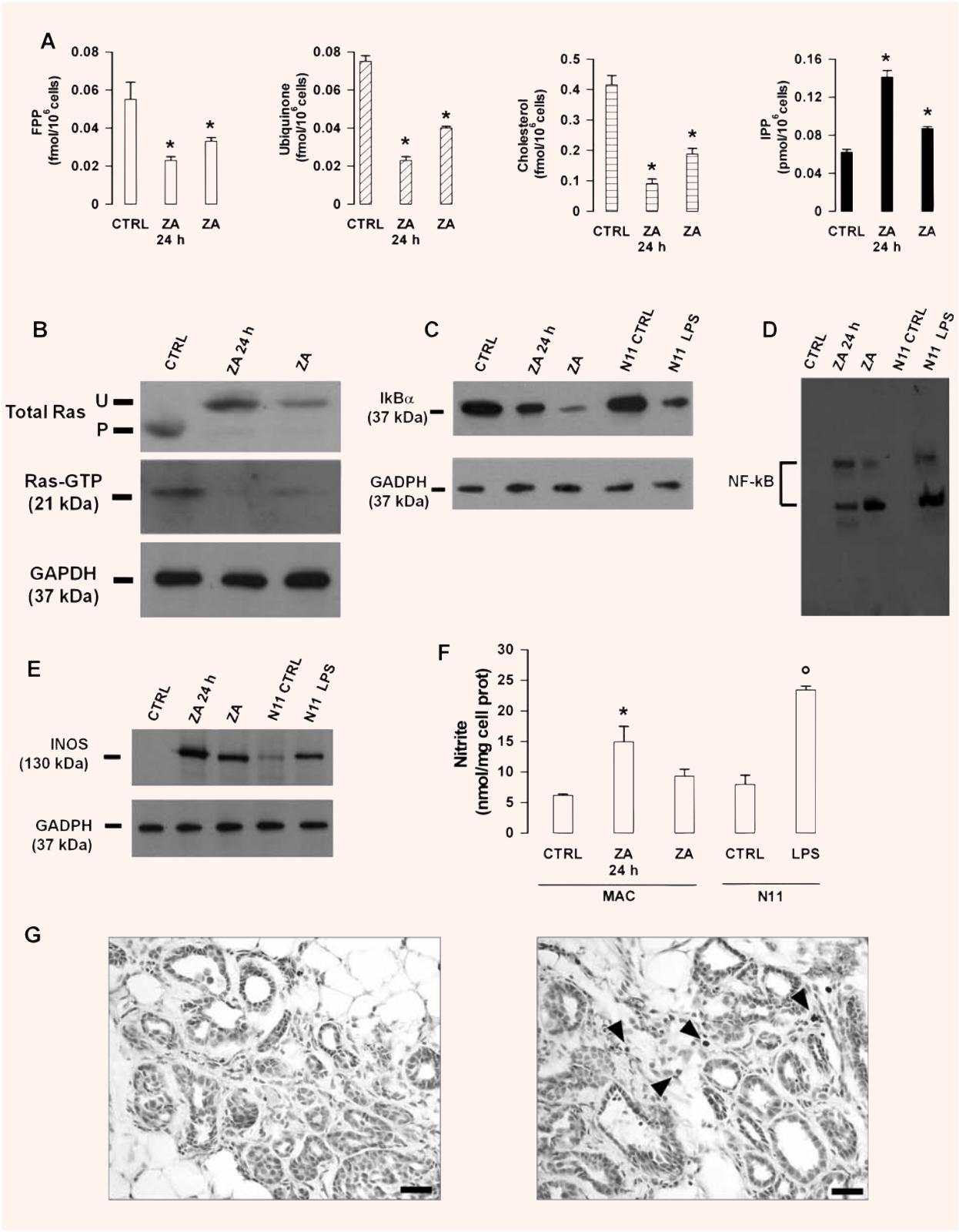

Fig. 5 Modulation of macrophages functions by low-dose ZA. Cells were isolated from control BALB-neuT mice and left untreated (CTRL) or treated *ex vivo* for 24 hrs with 1 μM ZA (ZA 24 hrs), or isolated from ZA-treated mice (ZA) as reported in the 'Materials and methods' section. (**A**) Inhibition of FPP synthase. A dose-dependent reduction of intracellular FPP, ubiquinone and cholesterol (always $*P < 0.01$, Student's t-test), together with a significant increase of IPP ($*P < 0.05$, Student's t-test) were displayed by ZA 24 hrs and ZA macrophages as compared to CTRL macrophages. Results are shown as mean ± S.E.M. of three experiments. (**B**) Inhibition of Ras prenylation and Ras activity. Ras pull-down assay and band shift assay in CTRL, ZA 24 hrs and ZA macrophages. (**C**, **D**) Activation of NF-κB. (**C**) Western blot analysis of IκB and GAPDH in CTRL, ZA 24 hrs and ZA macrophages. N11 glial cells cultured with (LPS N11) or without (CTRL N11) LPS 20 μg/ml were used as controls. (**D**) NF-κB translocation detected by EMSA on nuclear extracts from cell preparations run in lanes labelled as in (**C**). (**E**, **F**) Induction of iNOS expression and nitrite production. (**E**) Western blot analysis of iNOS and GAPDH in protein lysates from cell preparations run in lanes labelled as in (**C** and **D**). Results shown in (**B–E**) are from one representative out of three experiments. (**F**) Nitrite secretion by CTRL, ZA 24 hrs and ZA macrophages (MAC). Untreated (N11 CTRL) or LPS-treated (N11 LPS) N11 glial cells were used as controls. Results are expressed as mean ± S.E.M. of three experiments. The difference between ZA 24 hrs and CTRL macrophages is statistically significant ($*P < 0.01$, Student's t-test). (**G**) Nitrotyrosine expression (arrowheads) in the tumour stroma of ZA-treated (right panel) *versus* control (left panel) BALB-neuT mice. Scale bars, 40 μm.

Expression of iNOS is considered a hallmark of M1 polarized macrophages [32, 33]. iNOS is negatively regulated by the Mev pathway [34] and positively regulated by NF-κB [32, 35]. We thus evaluated ZA's ability to inhibit the Mev pathway and induce NF-κB-mediated iNOS expression in *ex vivo* and *in vivo* ZA-treated peritoneal macrophages. A significant reduction in the amount of FPP, ubiquinone and cholesterol, and a significant increase in the intracellular concentration of IPP was observed in both sets of macrophages, a confirmatory evidence of ZA's ability to specifically inhibit the FPP synthase (Fig. 5A).

Western blot analysis showed that Ras prenylation and Ras-GTP levels were greatly decreased in both *ex vivo* and *in vivo* ZA-treated macrophages (Fig. 5B). These changes were paralleled by a marked reduction in the expression of the inhibitory molecule IκB (Fig. 5C), and an increased translocation of NF-κB to the nucleus (Fig. 5D). Nuclear translocation of NF-κB is known to regulate iNOS expression [33, 35]. Macrophages freshly isolated from control mice did not express iNOS (Fig. 5E), and hence did not produce a significant amount of nitrites, which are stable derivatives of nitric oxide produced by iNOS (Fig. 5F). By contrast, a strong induction of iNOS expression and a significant increase in the secretion of nitrites were displayed by *ex vivo* and *in vivo* ZA-treated macrophages (Fig. 5E and F).

Nitration of tyrosine residues in tissue proteins is considered an *in vivo* marker of iNOS induction and local nitric oxide production [36]. Nitrotyrosine residues were detected by immunohistochemical staining in the tumour stroma of ZA-treated mice, whereas they were undetectable in control mice (Fig. 5G). These results provide a confirmatory evidence of *in vivo* ZA's ability to induce iNOS expression and nitric oxide production in TAMs.

Discussion

No data are available on the activity of ZA at clinically compatible doses in tumours not located in bone. In the present work, we show that ZA at doses approved for clinical use in human beings delays tumour development and prolongs disease-free and overall survival in BALB-neuT mice. Mice received ZA weekly at 100 μg/kg from the commercial clinical vial (free acid monohydrate). This formulation has a lower molecular weight than the pure research-grade substance (disodium salt), and hence the dose was even lower than the clinical 4 mg dose currently approved for the treatment of bone lesions or hypercalcaemia [17]. The mean cumulative number of doses (16 per mouse) was within the range recommended in human beings by clinical societies like ASCO [37].

This is the first study showing that ZA at clinically achievable doses has an impact on disease-free survival, and overall survival in a mouse model of primary tumour not located in bone. Reiterated low doses can be particularly effective in the treatment of extra-osseous malignancies where they can compensate for the rapid uptake of ZA in the bone, and enable a local effect both on tumour cells and neighbouring cells [8, 9, 17]. Notably, these results were observed only when ZA administration was started early during the ErbB-2 driven mammary carcinogenesis. ZA becomes ineffective if started when *in situ* carcinomas had progressed and the angiogenic switch that accompanies the progression to invasive cancer has already taken place (data not shown) [11].

It is very unlikely that ZA had a direct effect on tumour cell survival and proliferation *in vivo*, since the growth rate of TUBO cells, a cloned line derived from a mammary tumour of a BALB-neuT mouse [22], was affected *in vitro* after 5 days exposure to ZA concentrations from 10 to 100 times higher than those achievable *in vivo*. Indeed, most reports have shown that ZA has a direct antitumour activity *in vitro* at concentrations ranging from 50 μM to 1 mM, whereas lower concentrations are conceded if ZA is given in combination with standard anti-neoplastic agents [38, 39], or molecularly targeted agents, such as imatinib and tipifarnib [15, 40, 41].

Although high concentrations are required to affect TUBO cells growth, ZA concentrations around 1 μM are sufficient to inhibit FPP synthase and modulate the Mev pathway, as shown by the intracellular decrease of FPP, cholesterol and ubiquinone, and the concurrent increase of IPP. Notably, FPP synthase inhibition was marked enough to affect protein prenylation, as shown by the emergence of unprenylated Ras and the decreased intracellular

content of Ras-GTP in TUBO cells. The functional consequences of this defective protein prenylation in tumour cells are not completely understood, although a diminished production of proinflammatory chemokines and cytokines in response to Ras activation has been proposed [42]. These soluble factors play an important role in the local recruitment and activation of inflammatory cells and endothelial cells. Indeed, ZA-treated mice displayed a significant decrease in the number of TAMs, and this was paralleled by a significant decrease in tumour vascularization.

The local supply of VEGF was drastically cut off in both tumour cells and TAMs of ZA-treated mice, indicating a potent anti-angiogenic modulation of the tumour microenvironment. Even if ZA at high doses inhibits vascular endothelial cell functions *in vitro* and *in vivo*, its anti-angiogenic activity has been referred more to the activity on neighbouring cells like osteoclasts and TAMs than to direct apoptosis of endothelial cells [10, 11, 14].

The clinically compatible doses of ZA used in our study add further weight to the role of TAMs as critical targets bridging ZA-mediated antitumour and anti-angiogenic activity. Given their high endocytic activity, similar to that of osteoclasts with whom they share the same ontogeny, TAMs are in a privileged position to internalize ZA, even at the low concentrations they were exposed to in BALB-neuT mice. Indeed, we have previously shown that ZA at concentrations ranging from 0.5 to 1 μM deeply modulate the Mev pathway of monocytes and monocyte-derived dendritic cells [6].

Views about the role of TAMs in the tumour microenvironment have changed when they were found to display a polarized M2 phenotype and to sustain tumour growth and metastasis by reprogramming the local microenvironment and host immunity in favour of tumour cells [31–33]. Indeed, TAMs of control mice presented a polarized M2 phenotype, as shown by the expression of VEGF and IL-10, lack of IFN-γ production and concurrent NF-κB and iNOS down-regulation. This M2 polarization was reversed by ZA treatment which aborted IL-10 and VEGF production and recovered IFN-γ release in the mammary glands of ZA-treated mice. Autocrine and paracrine IFN-γ production is essential to generate M1 macrophages with immunostimulatory and tumoricidal functions [31, 32], and this presumption was formally proved by the lack of efficacy of ZA treatment in IFN-γ KO transgenic mice.

LPS and IFN-γ induce iNOS expression in macrophages by activating the NF-κB and STAT signalling pathways [31, 35]. iNOS is considered a hallmark of M1 macrophages [33] and its expression is inhibited by GTPase signalling proteins [34], which require prenylation to exert their regulatory function. Conversely, NF-κB is down-modulated in TAMs from mammary tumour-bearing mice and this is a key event downstream the IL-10 signalling pathway leading to reduced iNOS expression [43]. A marked inhibition of the Mev pathway was evident in *ex vivo* and *in vivo* ZA-treated peritoneal macrophages, as shown by the intracellular decrease of FPP, cholesterol and ubiquinone, and the concurrent increase of IPP. As expected, protein prenylation was also affected as shown by the decreased intracellular contents of prenylated Ras and Ras-GTP. ZA-mediated inhibition of the Mev pathway was paralleled by phosphorylation and inactivation of NF-κB bound IκB, and by the subsequent translocation of active NF-κB dimers into the nucleus, where they induced the expression of iNOS. Induction of iNOS was followed by a significant increase in the amount of nitrites, which are a well-known toxic intermediate with tumoricidal activity. The *in vivo* detection of nitrotyrosine residues in the tumour microenvironment is the proof-in-principle that TAMs recovered a M1 phenotype in ZA-treated mice.

Inhibition of FPP synthase by ZA was formally proven to induce the intracellular accumulation of IPP in both tumour cells and macrophages [44]. IPP is a phosphoantigen that stimulates the unique subset of Vγ9/Vδ2 T cells [45]. The antitumour potential of ZA in human beings has also been ascribed to stimulation of Vγ9/Vδ2 T cells *via* the accumulation of IPP in tumour cells [13] and antigen-presenting cells, such as monocytes and dendritic cells [6]. However, a murine counterpart of Vγ9/Vδ2 T cells has so far not been identified and we did not find any evidence of $\gamma\delta$ T-cell recruitment in the peripheral blood or lymphoid organs of ZA-treated mice (data not shown).

Our data point to TAMs as the most important immune target of ZA-mediated antitumour activity, and further support the idea that pharmacological skewing of TAMs polarization from M2 to a full M1 phenotype is an important element in solving the therapeutic conundrum of early treatment in cancer. Early recovery of M1-polarized functions can be less hazardous for the host than late attainment in the presence of a large tumour burden, when tumour cells, eventually killed by an effective antitumour immune response, can release factors turning TAMs back to a M2 phenotype.

The beneficial effects induced by ZA were not permanent, but they clearly establish a window opportunity for further therapeutic interventions. From the ethical standpoint, these strategies cannot include conventional chemotherapy agents because treatment is given at the hyperplastic stage and not at the stage of full-blown tumours. One choice could be to exploit the favourable immunologic setting established by ZA and further boost innate and/or adaptive antitumour immune responses by means of IL-12 [46], NKT stimulation with the glycolipid αGalCer [47], tumour-specific vaccination [11, 20] or depletion of Foxp3$^+$GITR$^+$ Treg cells or other suppressor cells [48].

In conclusion, our data indicate that administration of clinically compatible doses of ZA is an effective way of targeting hyperplastic cells and TAMs by switching the local microenvironment from a highly permissive partner to a tumour-hostile counterpart. The recent report by Gnant *et al.* provides clinical legitimation of our findings: a significant increase of disease-free survival has been observed in women with early-stage breast cancer after surgical removal and treatment with ZA in association with tamoxifene and aromatase as compared to those treated with the same regimen without ZA [49]. Given that tumour cells are lacking or minimally represented in these patients, the clinical efficacy of ZA should be ascribed to its ability to rebuild a healthier microenvironment with a reborn capacity to hamper tumour growth.

Acknowledgements

This work was supported in part by Ministero dell'Università e della Ricerca Scientifica (MIUR); Regione Piemonte, (Ricerca Sanitaria e Ricerca Scientifica); Compagnia San Paolo di Torino; Fondazione Neoplasie Sangue (Fo.Ne.Sa), Torino; the Italian Association for Cancer Research (AIRC); Fondazione C. Denegri; EC FP6 funding – EICOSANOX Project-LSHM-CT-2004–0050333 and this study was funded under the auspices of EUCAAD 200755. The project EUCAAD has received funding from the European Community's Seventh Framework Programme. We also would like to thank Raffaello Bertieri and Gino Boano (Novartis) for providing ZA.

Supporting Information

Additional Supporting Information may be found in the online version of this article.

Fig. S1 Zoledronic acid (ZA) treatment decreases spontaneous lung metastasis. Spontaneous lung metastasis was evaluated in control (grey bars, $n = 5$) and ZA-treated (solid bars, $n = 5$) mice. Data represent mean values ± S.E.M. of lung metastatic areas. A smaller metastatic area was already detectable in ZA-treated mice at 28 weeks of age ($*P = 0.06$, Student's t-test), a difference that became significant at 30 weeks ($**P = 0.01$, Student's t-test).

Fig. S2 Repeated administrations of clinically compatible doses of ZA are safe and do not induce organ damage. Organ damage was evaluated in ZA-treated mice after 4, 8 and 12 administrations of ZA at doses equivalent to those approved for clinical use in human beings. ZA-treated mice never showed any sign of organ damage as compared to control mice. Histological analysis of kidney (**a**) and colon (**b**) from a representative 25-week-old BALB-neuT mouse after 12 ZA administrations.

Fig. S3 Repeated administrations of clinically compatible doses of ZA increase bone density. Bone density was evaluated by micro-computed tomography (microCT) scan of the tibia in control (**a**) and ZA-treated (**b**) mice. As expected, a marked increase in bone density was already evident after eight administrations of ZA at clinically compatible doses.

Fig. S4 Decreased vascular endothelial growth factor (VEGF) serum levels in ZA-treated mice. The levels of circulating VEGF were assessed in sera of control and ZA-treated mice 1 week after the second ZA course. ZA-treated mice (solid bar, $n = 7$) showed significantly lower serum VEGF levels than control mice (grey bar, $n = 5$) ($P = 0.03$, Student's t-test). Results are expressed as mean values ± S.E.M.

Supporting Information methods

Evaluation of lung metastases. ZA-treated and control mice were evaluated for spontaneous lung metastases at 28 and 30 weeks of age. To optimize the detection of microscopic metastases and ensure systematic uniform and random sampling, lungs were processed as previously described [19]. Images of the entire lung tissue sections were acquired with a Leica DC500 camera at ×200 and analysed with the Adobe Photoshop program. The Lasso tool was used to delimit the surface occupied by metastases and their areas were recorded in pixels. The total area of metastases was evaluated in five mice per group. Groups were compared with a non-parametric test (Mann-Whitney test).

Evaluation of organ toxicity. Histological analysis of kidneys and colon were performed in groups of three ZA-treated mice after 4, 8 and 12 administrations of clinically compatible doses, and compared with three age-matched control mice. Cryo-sections were stained with haematoxylin and eosin, and histological and morphological evaluations were conducted by two pathologists blind to treatment group.

Microcomputed tomography imaging. After two courses of saline or ZA administration, 18-week-old BALB-neuT mice (3 from each group) were killed and their proximal tibia were evaluated by microCT for bone density. MicroCT analyses were also performed on tibia of BALB/c mice as a control (data not shown). MicroCT analyses were carried out by using a Skyscan 1172 X-ray-computed microtomograph (Skyscan, Kontich, Belgium), imaged with an X-ray tube voltage of 49 kV, current 200 μA and a 0.5 mm aluminium filter. The image pixel size was set to 4.37 μm. The scanning was initiated from the top of proximal tibia and continued for 4.085 mm. For each sample, a stack of 275 section images was reconstructed with the NRecon software (version 1.4.3, Skyscan). After reconstruction, the volume of interest (VOI) was designed by drawing interactively polygons on the 2D acquisition images. For trabecular bone measurement, the VOI was comprised only of cancellous bone, and the cortices were excluded. Trabecular fraction (BV/TV) was calculated covering 1 mm, starting from the lowest part of the growth plate (reference point). BV/TV is the ratio of the volume of bone present (BV) to the volume of the cancellous space (*i.e.* TV representing the VOI). For cortical bone measurement, the VOI was comprised only of the cortices, and the cancellous bone was excluded. Cortical bone volume (mm^3) was calculated covering 1.5 mm, starting 1.5 mm below the reference point. 3D modelling and analysis of the bone were obtained with the CTAn (version 1.5.0.2, Skyscan) and CTvol (version 1.9.4.1, Skyscan) software.

Serum VEGF detection. Blood samples from five saline-treated and seven ZA-treated BALB-neuT mice were collected from the retroorbital sinus and allowed to clot at room temperature for 1 hr. After centrifugation at 1.800 rpm for 10 min., serum was transferred, aliquoted and stored at -20°C until assayed. The presence of VEGF in each serum was evaluated by a multiplexed, particle-based, flow cytometric assay (Bioplex Protein Array System, Bio-Rad Laboratories S.r.l., Milano, Italy).

Please note: Wiley-Blackwell are not responsible for the content or functionality of any supporting materials supplied by the authors. Any queries (other than missing material) should be directed to the corresponding author for the article.

References

1. **Hillner BE, Ingle JN, Berenson JR, *et al.*** American Society of Clinical Oncology guideline on the role of bisphosphonates in breast cancer. American Society of Clinical Oncology Bisphosphonates Expert Panel. *J Clin Oncol.* 2000; 18: 1378–91.
2. **Roelofs AJ, Thompson K, Gordon S, *et al.*** Molecular mechanisms of action of bisphosphonates: current status. *Clin Cancer Res.* 2006; 12: 6222s-30s.
3. **Benford HL, Frith JC, Auriola S, *et al.*** Farnesol and geranylgeraniol prevent activation of caspases by aminobisphosphonates: biochemical evidence for two distinct pharmacological classes of bisphosphonate drugs. *Mol Pharmacol.* 1999; 56: 131–40.
4. **Benford HL, McGowan NW, Helfrich MH, *et al.*** Visualization of bisphosphonate-induced caspase-3 activity in apoptotic osteoclasts in vitro. *Bone.* 2001; 28: 465–73.
5. **Wolf AM, Rumpold H, Tilg H, *et al.*** The effect of zoledronic acid on the function and differentiation of myeloid cells. *Haematologica.* 2006; 91: 1165–71.
6. **Fiore F, Castella B, Nuschak B, *et al.*** Enhanced ability of dendritic cells to stimulate innate and adaptive immunity on short-term incubation with zoledronic acid. *Blood.* 2007; 110: 921–7.
7. **Hasmim M, Bieler G, Rüegg C.** Zoledronate inhibits endothelial cell adhesion, migration and survival through the suppression of multiple, prenylation-dependent signaling pathways. *J Thromb Haemost.* 2007; 5: 166–73.
8. **Clèzardin P.** Anti-tumour activity of zoledronic acid. *Cancer Treat Rev.* 2005; 31: 1–8.
9. **Stresing V, Daubine F, Benzaid I, *et al.*** Bisphosphonates in cancer therapy. *Cancer Letters.* 2007; 257: 16–35.
10. **Giraudo E, Inoue M, Hanahan D.** An amino-bisphosphonate targets MMP-9-expressing macrophages and angiogenesis to impair cervical carcinogenesis. *J Clin Invest.* 2004; 114: 623–33.
11. **Melani C, Sangaletti S, Barazzetta FM, *et al.*** Amino-biphosphonate-mediated MMP-9 inhibition breaks the tumor-bone marrow axis responsible for myeloid-derived suppressor cell expansion and macrophage infiltration in tumor stroma. *Cancer Res.* 2007; 67: 11438–46.
12. **Dieli F, Gebbia N, Poccia F, *et al.*** Induction of gammadelta T-lymphocyte effector functions by bisphosphonate zoledronic acid in cancer patients in vivo. *Blood.* 2003; 102: 2310–1.
13. **Mariani S, Muraro M, Pantaleoni F, *et al.*** Effector gammadelta T cells and tumor cells as immune targets of zoledronic acid in multiple myeloma. *Leukemia.* 2005; 4: 664–70.
14. **Croucher PI, De Hendrik R, Perry MJ, *et al.*** Zoledronic acid treatment of 5T2MM-bearing mice inhibits the development of myeloma bone disease: evidence for decreased osteolysis, tumor burden and angiogenesis, and increased survival. *J Bone Miner Res.* 2003; 18: 482–92.
15. **Kuroda J, Kimura S, Segawa H, *et al.*** The third-generation bisphosphonate zoledronate synergistically augments the anti-Ph^+ leukemia activity of imatinib mesylate. *Blood.* 2003; 102: 2229–35.
16. **Matsumoto S, Kimura S, Segawa H, *et al.*** Efficacy of the third-generation bisphosphonate, zoledronic acid alone and combined with anti-cancer agents against small cell lung cancer cell lines. *Lung Cancer.* 2005; 47: 31–9.
17. **Daubiné F, Le Gall C, Gasser J, *et al.*** Antitumor effects of clinical dosing regimens of bisphosphonates in experimental breast cancer bone metastasis. *J Natl Cancer Inst.* 2007; 99: 322–30.
18. **Boggio K, Nicoletti G, Di Carlo E, *et al.*** Interleukin 12-mediated prevention of spontaneous mammary adenocarcinomas in two lines of Her-2/neu transgenic mice. *J Exp Med.* 1998; 188: 589–96.
19. **Di Carlo E, Diodoro MG, Boggio K, *et al.*** Analysis of mammary carcinoma onset and progression in HER-2/neu oncogene transgenic mice reveals a lobular origin. *Lab Invest.* 1999; 79: 1261–9.
20. **Quaglino E, Iezzi M, Mastini C, *et al.*** Electroporated DNA vaccine clears away multifocal mammary carcinomas in her-2/neu transgenic mice. *Cancer Res.* 2004; 64: 2858–64.
21. **Hüsemann Y, Geigl JB, Schubert F, *et al.*** Systemic spread is an early step in breast cancer. *Cancer Cell.* 2008; 13: 58–68.
22. **Rovero S, Amici A, Carlo ED, *et al.*** DNA vaccination against rat her-2/Neu p185 more effectively inhibits carcinogenesis than transplantable carcinomas in transgenic BALB/c mice. *J Immunol.* 2000; 165: 5133–42.
23. **Righi M, Mori L, De Libero G, *et al.*** Monokine production by microglial cell clones. *Eur J Immunol.* 1989; 19: 1443–8.
24. **Seifert SC, Lucas JJ.** Incorporation of mevalonate into dolichol and other isoprenoids during estrogen-induced chick oviduct differentiation. *Biochim Biophys Acta.* 1988; 962: 16–24.
25. **Lobell RB, Omer CA, Abrams MT, *et al.*** Evaluation of Farnesyl:protein transferase and geranylgeranyl:protein transferase inhibitor combinations in preclinical models. *Cancer Res.* 2001; 61: 8758–68.
26. **Danen EH, Sonneveld P, Sonnenberg A, *et al.*** Dual stimulation of Ras/mitogen-activated protein kinase and RhoA by cell adhesion to fibronectin supports growth factor-stimulated cell cycle progression. *J Cell Biol.* 2000; 151: 1413–22.
27. **Riganti C, Orecchia S, Pescarmona G, *et al.*** Statins revert doxorubicin resistance via nitric oxide in malignant mesothelioma. *Int J Cancer.* 2006; 119: 17–27.
28. **Ghigo D, Aldieri E, Todde R, *et al.*** Chloroquine stimulates nitric oxide synthesis in murine, porcine, and human endothelial cells. *J Clin Invest.* 1998; 102: 595–605.
29. **Nanni P, Nicoletti G, Palladini A, *et al.*** Antimetastatic activity of a preventive cancer vaccine. *Cancer Res.* 2007; 67: 11037–44.
30. **Winter MC, Holen I, Coleman RE.** Exploring the anti-tumour activity of bisphosphonates in early breast cancer. *Cancer Treat Rev.* 2008; 34: 453–75.
31. **Sica A, Schioppa T, Mantovani A, *et al.*** Tumour-associated macrophages are a distinct M2 polarised population promoting tumour progression: potential targets of anti-cancer therapy. *Eur J Cancer.* 2006; 42: 717–27.
32. **Sica A, Bronte V.** Altered macrophage differentiation and immune dysfunction in tumor development. *J Clin Invest.* 2007; 117: 1155–66.
33. **Weigert A, Brüne B.** Nitric oxide, apoptosis and macrophage polarization during tumor progression. *Nitric Oxide.* 2008; 19: 95–102.
34. **Zuckerbraun BS, Barbato JE, Hamilton A, *et al.*** Inhibition of geranylgeranyltransferase I decreases generation of vascular reactive oxygen species and increases vascular nitric oxide production. *J Surg Res.* 2005; 124: 256–63.
35. **Aktan F.** iNOS-mediated nitric oxide production and its regulation. *Life Sci.* 2004; 75: 639–53.

36. **Heijnen HF, van Donselaar E, Slot JW, *et al.*** Subcellular localization of tyrosine-nitrated proteins is dictated by reactive oxygen species generating enzymes and by proximity to nitric oxide synthase. *Free Radic Biol Med.* 2006; 40: 1903–13.
37. **Kyle RA, Yee GC, Somerfield MR, *et al.*** American Society of Clinical Oncology 2007 clinical practice guideline update on the role of bisphosphonates in multiple myeloma. *J Clin Oncol.* 2007; 25: 2464–72.
38. **Woodward JK, Coleman RE, Holen I.** Preclinical evidence for the effect of bisphosphonates and cytotoxic drugs on tumor cell invasion. *Anticancer Drugs.* 2005; 16: 11–9.
39. **Ottewell PD, Mönkkönen H, Jones M, *et al.*** Antitumor effects of doxorubicin followed by zoledronic acid in a mouse model of breast cancer. *J Natl Cancer Inst.* 2008; 100: 1167–78.
40. **Kim SJ, Uehara H, Yazici S, *et al.*** Modulation of bone microenvironment with zoledronate enhances the therapeutic effects of STI571 and paclitaxel against experimental bone metastasis of human prostate cancer. *Cancer Res.* 2005; 65: 3707–15.
41. **Caraglia M, Marra M, Leonetti C, *et al.*** R115777 (Zarnestra)/Zoledronic acid (Zometa) cooperation on inhibition of prostate cancer proliferation is paralleled by Erk/Akt inactivation and reduced Bcl-2 and bad phosphorylation. *J Cell Physiol.* 2007; 211: 533–43.
42. **Borrello MG, Degl'Innocenti D, Pierotti MA.** Inflammation and cancer: the oncogene-driven connection. *Cancer Lett.* 2008; 267: 262–70.
43. **Sica A, Saccani A, Bottazzi B, *et al.*** Autocrine production of IL-10 mediates defective IL-12 production and NF-kappa B activation in tumor-associated macrophages. *J Immunol.* 2000; 164: 762–7.
44. **Mönkkönen H, Ottewell PD, Kuokkanen J, *et al.*** Zoledronic acid-induced IPP/Appl production *in vivo*. *Life Sci.* 2007; 81: 1066–70.
45. **Constant P, Davodeau F, Peyrat MA, *et al.*** Stimulation of human gamma delta T cells by nonpeptidic mycobacterial ligands. *Science.* 1994; 264: 267–70.
46. **Cifaldi L, Quaglino E, Di Carlo E, *et al.*** A light, nontoxic interleukin 12 protocol inhibits HER-2/neu mammary carcinogenesis in BALB/c transgenic mice with established hyperplasia. *Cancer Res.* 2001; 61: 2809–12.
47. **Hayakawa Y, Rovero S, Forni G, *et al.*** Alpha-galactosylceramide (KRN7000) suppression of chemical- and oncogene-dependent carcinogenesis. *Proc Natl Acad Sci USA.* 2003; 100: 9464–9.
48. **Curiel TJ.** Regulatory T cells and treatment of cancer. *Curr Opin Immunol.* 2008; 20: 241–6.
49. **Gnant M, Mlineritsch B, Schippinger W, *et al.*** Endocrine therapy plus zoledronic acid in premenopausal breast cancer. *N Engl J Med.* 2009; 360: 679–91.